Pol. J. Environ. Stud. Vol. XX, No. X (XXXX), 1-18
DOI: *10.15244/pjoes/207057* ONLINE PUBLICATION DATE: 2025-09-19

Original Research

Multi-Scenario Simulation of Habitat Quality in the Yellow River Basin by Coupling FLUS with InVEST Model

Ning Xu[1], Zhike Zhou[2], Zhiguo Li[1]*, Shun Zhang[1], Xinyu Dong[1], Xinyu Zhu[1], Mengyao Wan[1], Zhen He[1]

[1]Henan Engineering Technology Research Center of Ecological Protection and Management of the Old Course of Yellow River & Henan Green Technology Innovation Demonstration Base, Shangqiu Normal University, Shangqiu, 476000, China
[2]School of Geographical Sciences, Hebei Normal University, Shijiazhuang 050024, China

Received: 21 February 2025
Accepted: 12 June 2025

Abstract

Current research on the relationship between land use change and habitat quality and the driving factors, interactions, and future changes under multi-scenarios remains limited, especially in the ecologically fragile Yellow River Basin (YRB). Using the 2000, 2010, and 2020 land use data, we coupled FLUS with the InVEST model to analyze the relationship between land use change and habitat quality and predict habitat quality under 4 development scenarios. The driving factors were quantitatively identified by their interactive effects by utilizing Geodetector. The results showed that: (1) Overall, habitat quality of the YRB was moderate with an improving trend but exhibited significant spatial heterogeneity. The spatial distribution of habitat quality aligned closely with land use patterns. Habitat degradation showed a spatial pattern of "central-high, peripheral-low; eastern-high, western-low". (2) Land use was the primary driver of habitat quality differentiation ($q > 0.8$), with population density and GDP gaining influence. Factor interactions, especially between land use and other variables, exceeded individual effects. (3) Under the ecological space priority scenario, habitat quality improves significantly, especially in fragile zones where policy interventions are effective. Conversely, the production space priority scenario risks habitat degradation, necessitating measures to mitigate ecological pressure caused by industrial mining and urban expansion.

Keywords: InVEST model, FLUS model, geodetector, habitat quality

Introduction

Habitat refers to the natural environment that provides living space for humans and other species [1]. Habitat quality is the capacity of an ecosystem to offer suitable conditions for the continuous survival of individuals and populations [2, 3], and it reflects

*e-mail: lizhiguo@sqnu.edu.cn
Tel.: +86-15836877176

the biodiversity status of a region, which is often dependent on the intensity of human activities [4]. Currently, habitat quality is under increasing threat from human activities. Therefore, evaluating the current state of habitat quality and its trends is crucial for studying biodiversity and its conservation. Land use directly reflects human activities, represents the combined effects of natural and anthropogenic factors, and is one of the most critical determinants of habitat quality [5, 6]. It alters the composition and structure of habitats and ultimately affects the flow of materials and energy between patches [7]. Frequent human activities degrade habitat quality, reduce landscape connectivity, and intensify land fragmentation, causing significant damage to regional habitat quality [8].

In recent years, on the spatial scale of research objects, scholars have evaluated the habitat quality related to countries [9, 10], provinces [11, 12], basins [13-15], cities [16], coastal zones [17], and typical ecological reserves [18, 19]. Currently, field surveys and model-based evaluations are two main approaches for assessing habitat quality [18]. Some researchers primarily assess the quality of wildlife habitats through biodiversity and habitat field surveys by constructing evaluation indicator systems [20, 21]. Still, this method is time-consuming and labor-intensive, making it challenging to apply in large-scale areas. Consequently, the model-based evaluation methods have emerged due to their simplicity and ease of use, gradually replacing traditional approaches and gaining widespread adoption among scholars. Some of the commonly used models include the SoLVES model [22], the ARIES model [13], the Maxent model [19], and the InVEST model [10-17]. Among them, the InVEST model calculates habitat quality by linking threat factors to land use types and determining the impact of threat factors on habitat, thereby assessing regional environmental quality [23]. The InVEST model is widely used due to its low parameter requirements, ease of data acquisition, simple operation, and highly accurate analytical capabilities [24].

Domestically and internationally, scholars have carried out spatial-temporal simulations of land use under multi-scenarios to analyze future land use changes. Among these, the Cellular Automata (CA) model is one of the most commonly used methods [25]. Based on the CA model, other models such as the CA-Markov [26], CLUE-S [27], and multi-agent models [28] have been developed. The FLUS model integrates the advantages of multiple traditional models, simplifying the system dynamics (SD) model construction process, overcoming the limitations of the CA model in simulating nonlinear systems, and addressing the inability of the Markov model to incorporate driving factors [29, 30]. It can provide highly accurate spatial land use change results, especially when simulating the complex mechanisms of multi-factor interactions in human-environment coupled systems and different land use type transitions [30]. With the increasing application of the FLUS model, more studies have focused on simulating and predicting land use changes.

Evaluating regional habitat quality based on land use, revealing its driving factors, and predicting future changes have become a key focus in research. However, there is no unified standard for evaluating habitat quality attributes and spatial changes caused by land use change [14]. Additionally, the studies available have not delved deeply enough into analyzing the influential factors and driving mechanisms of habitat quality changes. Most current studies have included natural and human factors in single-factor analysis models [9, 12, 14, 31], while few studies have comprehensively explored the natural and human factors influencing habitat quality and their interactive effects. Furthermore, in future land use prediction, many past studies mainly consider the impact of climate change on land use, establishing a single simulation scenario while often neglecting the dynamic feedback loops between development strategies and land use change [16, 32, 33]. The YRB, one of China's most ecologically and economically significant regions, has been under increasing pressure from both natural and anthropogenic activities [34]. Rapid urbanization, industrialization, and land use change have significantly transformed the YRB's habitat quality, leading to biodiversity loss and ecological degradation [35]. Ecological protection and governance in the Yellow River Basin are imperative. Therefore, this study analyzed the spatiotemporal variation of land use and habitat quality of the YRB from 2000 to 2020. The main objectives are to (1) analyze the spatial distribution pattern and evolutionary characteristics of land use and habitat quality; (2) quantitatively identify the key driving factors and their interactions influencing habitat quality by utilizing Geodetector; (3) simulate the spatial characteristics of future land use and habitat quality by coupling FLUS with the InVEST model under 4 distinct development scenarios in 2030 and 2050. This study can provide scientific support for optimizing land use structures, improving regional ecological quality, and guiding the implementation of ecological restoration projects in the basin.

Materials and Methods

Research Area Overview

The YRB is located in northern China, spanning between 95°53′31″ ~ 119°19′29″ E and 32°9′35″ ~ 41°50′23″ N (Fig. 1). It covers an area of approximately 8×10^5 km² and covers 9 provinces: Qinghai, Sichuan, Gansu, Ningxia, Inner Mongolia, Shaanxi, Shanxi, Henan, and Shandong [14]. It crosses four geomorphological units: the Tibetan Plateau, Inner Mongolia Plateau, Loess Plateau, and North China Plain, with high and low terrain in the west and east. The basin encompasses arid, semi-arid, and semi-humid climate zones, with a multi-year average

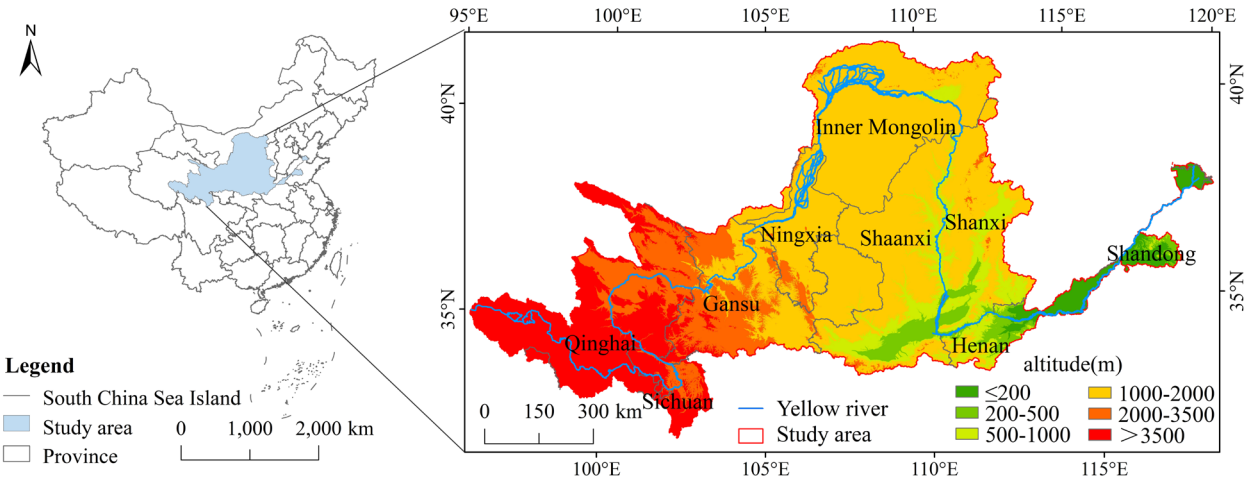

Fig. 1. Location of the study area.

temperature of around 7°C and an annual precipitation of approximately 440 mm. Both precipitation and temperature exhibit a decreasing spatial gradient from southeast to northwest. The YRB is also significant for population activity and economic development. By the end of 2020, the basin's population reached 420 million, with a regional Gross Domestic Product (GDP) of 2.39 trillion yuan. The region is currently undergoing rapid urbanization and industrialization, intensifying the contradiction between human activities and the environment [36]. Due to the complexity of its geomorphological units, significant climate variability, and frequent human activities, the YRB has become one of China's most ecologically fragile areas, facing severe problems such as soil erosion, land desertification, vegetation degradation, and biodiversity loss. It is urgently necessary to analyze the spatiotemporal differentiation characteristics of habitat quality driving factors and to predict future habitat quality under multi-scenarios.

Data

The data used in this study included land use, soil type, topography, climate, and socioeconomic factors of the YRB in 2000, 2010, and 2020. All data sources are listed in Table 1, with the coordinate system unified as Krasovsky_1940_Albers. We extracted altitude, slope, aspect, terrain niche index, and the relief degree of land surface (RDLS) utilizing ASTER GDEM v3. The terrain niche index and RDLS calculation methods refer to the relevant literature [37, 38].

Table 1. Location of the study area.

	Resolution	Data source
Boundary of the Yellow River Basin		https://www.ckcest.cn/home/
Land use	30 m*30 m	http://www.resdc.cn/
ASTER GDEM v3	30 m*30 m	http://www.gscloud.cn/
Soil type	1 km*1 km	http://www.resdc.cn/
Vegetation index	30 m*30 m	National Ecological Data Center Resource Sharing Service Platform http://www.nesdc.org.cn/
Annual average temperature	1 km*1 km	http://loess.geodata.cn/
Annual average precipitation	1 km*1 km	http://loess.geodata.cn/
Population density	1 km*1 km	https://landscan.ornl.gov/
GDP	1 km*1 km	https://data.tpdc.ac.cn/home
Impervious surface	30 m*30 m	Institute of Remote Sensinging, Wuhan University http://irsip.whu.edu.cn/resources/dataweb.php
Road		https://www.openstreetmap.org

Table 2. Habitat suitability and threat sensitivity in the YRB.

Land use type	Habitat suitability	Sensitivity of land use types to threats					
		Paddy field	Dryland	Urban Land	Rural residential area	Other construction land	Unused land
Paddy field	0.5	0.25	0.3	0.5	0.4	0.5	0.4
Dryland	0.4	0.3	0.25	0.5	0.4	0.5	0.4
Woodland	0.9	0.7	0.7	0.8	0.8	0.8	0.5
Shrubland	0.85	0.7	0.7	0.75	0.75	0.75	0.4
Sparse woodland	0.8	0.7	0.7	0.75	0.75	0.75	0.5
Other woodlands	0.8	0.7	0.7	0.7	0.7	0.7	0.4
High coverage grassland	0.7	0.6	0.7	0.5	0.5	0.35	0.5
Moderate coverage grassland	0.6	0.6	0.7	0.6	0.45	0.35	0.6
Low coverage grassland	0.5	0.35	0.35	0.5	0.4	0.35	0.7
Canals	0.3	0.2	0.2	0.3	0.3	0.3	0.1
Lakes	0.8	0.65	0.65	0.8	0.75	0.8	0.1
Reservoir pits	0.8	0.5	0.5	0.8	0.75	0.85	0.2
Foreshore	0.6	0.65	0.65	0.7	0.65	0.75	0.2
Overflow land	0.7	0.75	0.7	0.7	0.65	0.75	0.3
Urban land	0	0	0	0	0	0	0
Rural residential area	0	0	0	0	0	0	0
Other construction land	0	0	0	0	0	0	0
Unused land	0	0	0	0	0	0	0
Sea	0.8	0.5	0.5	0.8	0.65	0.75	0.2

Methods

InVEST Model

The habitat quality module of the InVEST model assumes that areas with higher habitat quality can support greater species richness, and habitat quality changes will lead to biodiversity changes [39]. The calculation of habitat quality requires four main components: the relative impact of each threat factor, the sensitivity of each land use type to each threat factor, the distance between land use and the source of the threat, and the degree of legal protection. The InVEST model equation is as follows [40]:

$$D_{xj} = \sum_{r=1}^{R} \sum_{y=1}^{Y_r} \left(\frac{w_r}{\sum_{r=1}^{R} w_r} \right) r_y i_{rxy} \beta_x S_{jr} \quad (1)$$

$$i_{rxj} = 1 - \left(\frac{d_{xy}}{d_{rmax}} \right) \text{ (linear decay)} \quad (2)$$

$$i_{rxy} = \exp\left(-\frac{2.99 d_{xy}}{d_{rmax}} \right) \text{ (exponential decay)} \quad (3)$$

where D_{xj}, R, W_r, Y_r, and r_y represent the habitat degradation index, the number of threat factors, the weight of threat factor r, the number of threat factor grids, and the value of threat factors on the grid, respectively. i_{rxy} represents the distance between habitat and threat sources and the spatial impact of threats. β_x is a factor that mitigates the effects of threats on habitats through various conservation policies. S_{jr} represents the sensitivity of habitat type j to threat factor r. d_{xy} is the straight-line distance between grids x and y, and d_{rmax} is the maximum influence range of threat factor r. The habitat quality can be estimated as follows:

$$Q_{xj} = H_j \left(1 - \left(\frac{D_{xj}^z}{D_{xj}^z + k^z} \right) \right) \quad (4)$$

where Q_{xj} represents the habitat quality index of grid x for land use type j; H_j represents the habitat suitability of habitat type j, with values ranging from 0 to 1; k is the half-saturation constant, typically set to half

Table 3. Threat factors and their degree of stress.

Threat factors	Weight	Maximum influence distance/km	Type of recession
Paddy field	0.6	4	Linear
Dryland	0.6	4	Linear
Urban land	1	10	Index
Rural residential area	0.7	5	Index
Other construction land	0.9	9	Index
Unused land	0.3	1	Linear

of the maximum habitat degradation value; and z is a normalization constant, usually set to 2.5 [40].

The inputs for this module primarily include land use data, major threat factors, the weights and impact distances of threat factors, and the sensitivity of each land use type to each threat source. Based on the InVEST model user guide and previous research [41-44], we specifically considered the distribution of nature reserves, the implementation of reforestation and grassland restoration policies, and the processes of industrialization and urbanization in the study area to ensure the model's applicability and accuracy. The selected threat factors include paddy fields, dryland, urban land, rural residential areas, other construction land, and unused land. The habitat suitability and threat sensitivity for each land use type are listed in Table 2, along with the relative weight of each threat factor, the maximum impact distance, and the type of spatial decay (Table 3).

FLUS Model

The FLUS model was employed to simulate the spatial distribution of land use. This model improves the traditional Markov chain model and incorporates suitability probability calculations, neighborhood factor calculations, adaptive inertia coefficient calculations, transition cost settings, and comprehensive probability calculations [30]. The suitability probability calculation uses a BP-ANN algorithm to fit the baseline land use types with various spatial driving factors, obtaining the suitability probability of different land use types [29, 30]. The expression for this is:

$$sp(p,k) = \sum_j W_{j,k} \times \frac{1}{1+e^{-N_i(p,q)}} \quad (5)$$

$$N_i(p,q) = \sum_i W_{i,j} \times x_i(p,q) \quad (6)$$

where $sp(p, k)$ is the suitability probability, $W_{j,k}$ is the weight between the hidden layer and the output layer, $N_i(p, q)$ represents the signal received by neuron j in the hidden layer from the input layer, $x_i(p, q)$ is the input value of cell p for neuron iii at iteration q, and $W_{i,j}$ is the weight between the input layer and the hidden layer. The neighborhood factor represents the interaction between land use types and land use cells within the neighborhood range. Its expression is:

$$\Omega^t_{p,k} = \frac{\sum con(c_p^{t-1} = k)}{\frac{N \times N}{N \times N - 1}} \times W_k \quad (7)$$

where $\Omega^t_{p,k}$ is the neighborhood influence factor of cell p at time t; $\sum_{N \times N} \mathrm{con}(c_p^{t-1}=k)$ represents the total number of

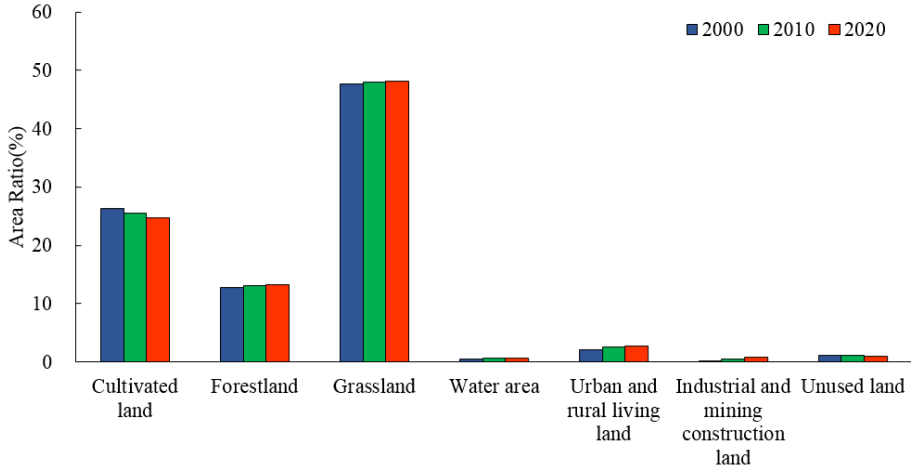

Fig. 2. Land use structure change in the YRB.

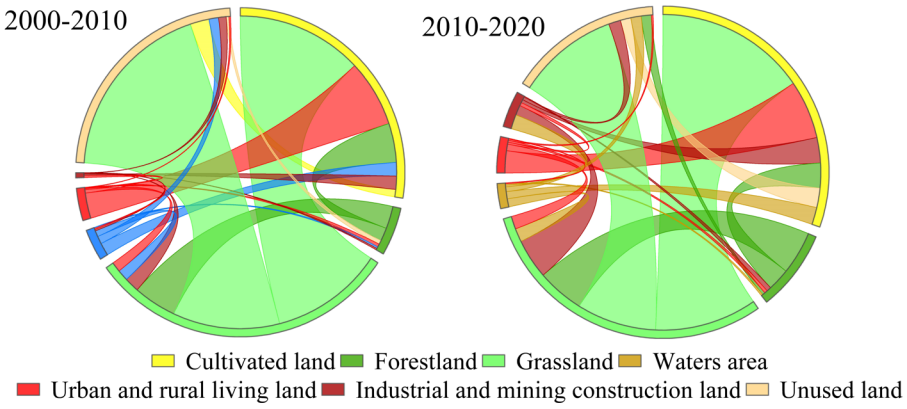

Fig. 3. Land use transfer of the YRB from 2000 to 2020.

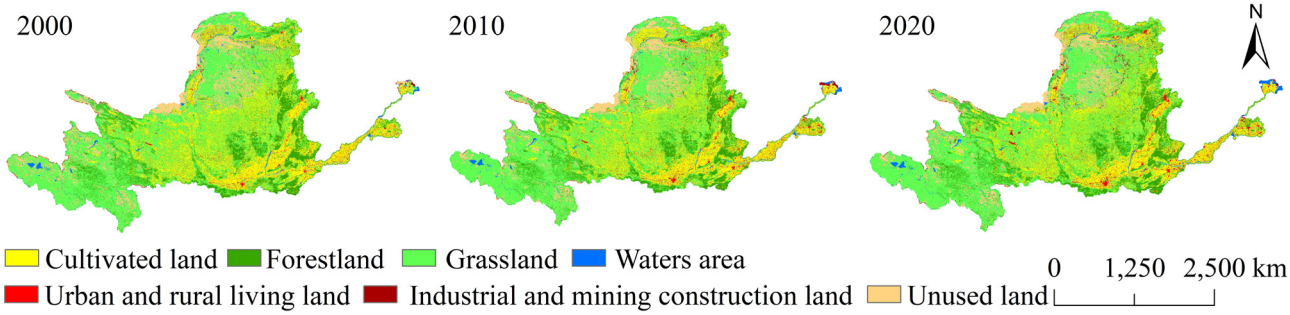

Fig. 4. Land use distribution map from 2000 to 2020.

cells of land use type k within the Moore neighborhood of $N \times N$ in the last iteration at time t - 1. W_k represents the neighborhood factor parameter for each land use type, with values ranging from 0 to 1, and the value is positively correlated with land use expansion capability.

Geodetector

The Geodetector is a new statistical method used to detect spatial heterogeneity and uncover the driving factors behind it. The single-factor and interaction detection methods can measure spatial heterogeneity, explore explanatory factors, and analyze the interaction between variables [45, 46]. Its expression is:

$$q = 1 - \frac{\sum_{h=1}^{L} N_h \sigma_h^2}{N\sigma^2} \quad (8)$$

where q represents the explanatory power of a factor on the spatiotemporal variation of habitat quality; h is the number of classifications or partitions of the factor; L refers to the stratification of the independent or dependent variable; N_h and N represent the number of units in layer h and the total number of units in the study area, respectively; and σ_h^2 and σ^2 are the variances of the independent variable factor and the dependent variable habitat quality spatiotemporal variation, respectively. The range of q values is [0, 1], with larger q values indicating stronger explanatory power of the independent variable factor for the spatiotemporal variation of habitat quality and smaller values indicating weaker explanatory power.

Considering the natural geographical characteristics and the intensity of human activities in the YRB, and based on relevant literature and expert opinions, we selected 14 driving factors: altitude (X1), slope (X2), aspect (X3), terrain niche index (X4), RDLS (X5), soil type (X6), vegetation coverage (X7), annual average temperature (X8), annual precipitation (X9), land use (X10), population density (X11), GDP (X12), impervious surfaces (X13), and road distance (X14). A systematic sampling of the YRB was conducted with a grid size of 500 m, resulting in a total of 3,255,852 sample points.

Results

Spatiotemporal Analysis of Land Use Changes

The land use changes in the YRB from 2000 to 2020 exhibit significant dominance and temporal and spatial variation characteristics. As shown in Fig. 2, grassland was the dominant land use type during the study period, accounting for more than 47% of the total area, followed by cultivated land and forestland. The combined area of grassland, cultivated land, and forestland accounted

for over 86% of the total, while other land use types occupied relatively more minor regions. From a temporal perspective, from 2000 to 2020, the areas of grassland, forestland, urban and rural living land, and industrial and mining construction land all showed a continuously increasing trend, with the most dramatic changes occurring in industrial and mining construction land (379.39% growth) and urban and rural living land (36.45% growth). In contrast, cultivated and unused land showed a continuous decreasing trend, with the most substantial reduction occurring in unused land, decreasing by 11.30%.

From 2000 to 2010, the new grassland area primarily originated from unused land and cultivated land, accounting for 53.52% and 37.03% of the total new grassland area, respectively (Fig. 3). The new forestland area mainly came from grassland and cultivated land, making up 49.93% and 45.18% of the total new forest area, respectively. The newly added water areas were primarily sourced from cultivated land, grassland, and unused land, accounting for 36.38%, 29.80%, and 25.80%, respectively. New urban and rural living land was mainly converted from cultivated land, contributing 79.17% of the newly added urban-rural residential area. The new industrial and mining construction land predominantly came from grassland and cultivated land, accounting for 37.08% and 33.34% of the total new industrial and mining construction land area, respectively. The land converted from cultivated land was mainly transformed into grassland and urban and rural living land, accounting for 47.43% and 25.10% of the total cultivated land area transferred. Unused land was mainly converted into grassland, accounting for 81.85%.

From 2010 to 2020, the new grassland area primarily originated from cultivated and unused land, making up 47.13% and 31.78% of the total new grassland area, respectively. New forestland was mainly sourced from grassland and cultivated land, accounting for 54.66% and 28.87%, respectively. The new water bodies were mainly sourced from cultivated land, industrial and mining construction land, and grassland, accounting for 29.78%, 25.01%, and 23.24%, respectively. The newly added urban and rural living land was predominantly sourced from cultivated land, which accounted for 72.93% of the total. New industrial and mining construction land came primarily from grassland and cultivated land, contributing 46.56% and 29.75%, respectively. The land converted out of cultivated land was primarily transformed into grassland and urban and rural living land, accounting for 50.96% and 19.73% of the total cultivated land area transferred. Unused land was mainly converted into grassland, accounting for 69.53% of the total area transferred from unused land.

From a spatial distribution perspective, grassland dominates the western and central parts of the YRB, forestland is predominant in the southern region, and cultivated land, urban and rural living land, and industrial and mining construction land are concentrated in the eastern part. Water bodies are scattered throughout the basin, while unused land is mainly distributed in the northwest (Fig. 4). Land use changes have exhibited significant spatial differentiation. Cultivated land has been converted to forestland and grassland, with these changes concentrated in the northeastern part of Inner Mongolia and northern Shanxi. Cultivated land has also been transformed into urban and rural living land, primarily in urban-rural fringe areas. Unused land has been converted to forestland and grassland, mainly concentrated in the northern part of the basin. The conversion of grassland to forestland has predominantly occurred in the upstream areas of the YRB. In contrast, grassland degradation into unused land has been concentrated in central Qinghai in the upper reaches of the Yellow River.

Habitat Quality and Degradation Analysis

Habitat Quality Analysis

The equal interval method was used to divide the scores into 5 levels of habitat quality status, including lower (0 ~ 0.2), low (0.2 ~ 0.4), middle (0.4 ~ 0.6), high (0.6 ~ 0.8), and higher (0.8 ~ 1.0). The average habitat quality values in 2000, 2010, and 2020 were 0.5052, 0.5069, and 0.5068, respectively, all within the middle range and showing an overall improving trend. Habitat quality of the YRB was predominantly at a middle level, followed by low and high levels. From a temporal perspective, the areas of high and higher habitats continuously increased, while those of low habitat quality decreased steadily. The area of middle habitat quality first decreased and then increased, while the area of lower habitat quality initially increased and then decreased. From a spatial distribution perspective, the overall habitat quality of the study area exhibited a pattern of high values in the western and southeastern regions, middle values in the central region, and low values in the northern region, which largely aligned with the distribution of land use (Fig. 5). The areas of higher value were primarily located in the southeastern part of the YRB, dominated by forestland. The area of high value was mainly distributed in the southwestern part of the basin, characterized by forestland, grassland, and water bodies. In contrast, lower and low habitat quality areas were concentrated in the eastern and northern parts of the basin, where urban and rural living land, industrial and mining land, and unused land were prevalent. The middle habitat quality area was mainly concentrated in the central part of the basin, primarily in grassland regions.

From 2000 to 2010, areas with declining habitat quality were mainly concentrated around the Weihe River Basin, the Yellow River Delta, and parts of Shaanxi, Sichuan, Qinghai, and Shanxi. Regions where habitat quality improved were scattered. From 2010 to 2020, areas with declining habitat quality were distributed more extensively but showed improvement

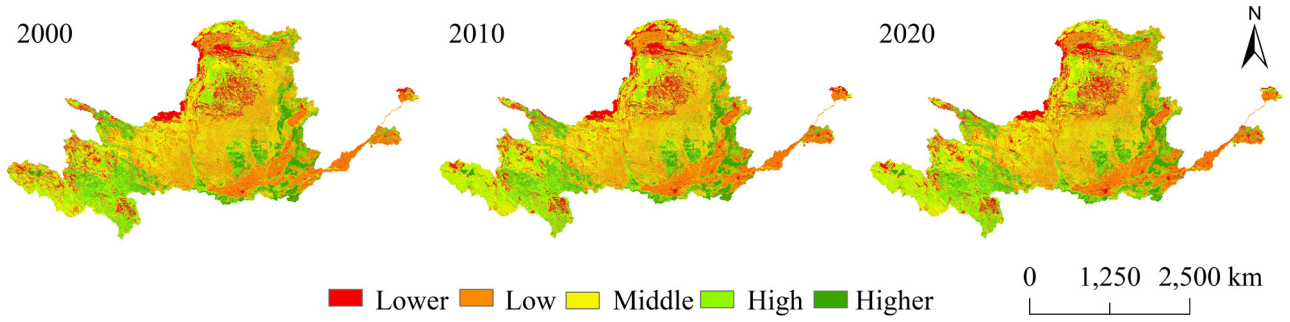

Fig. 5. Habitat quality classification map of the YRB from 2000 to 2020.

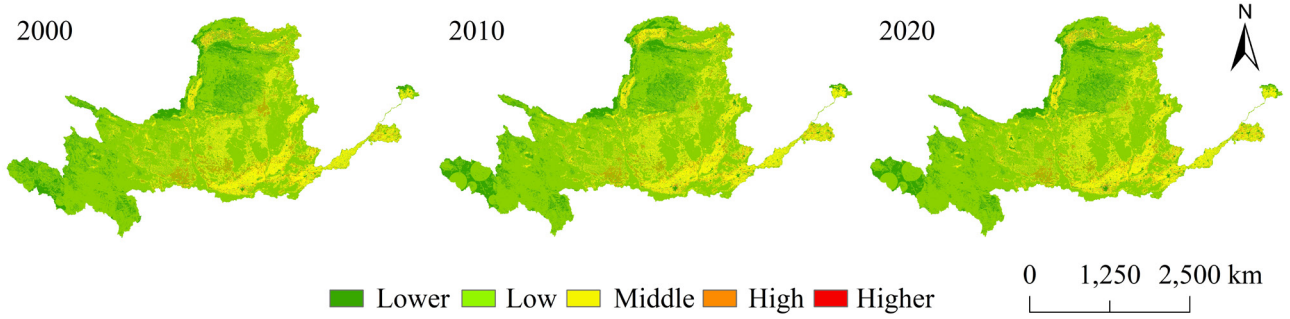

Fig. 6. Habitat quality degradation level map of the YRB from 2000 to 2020.

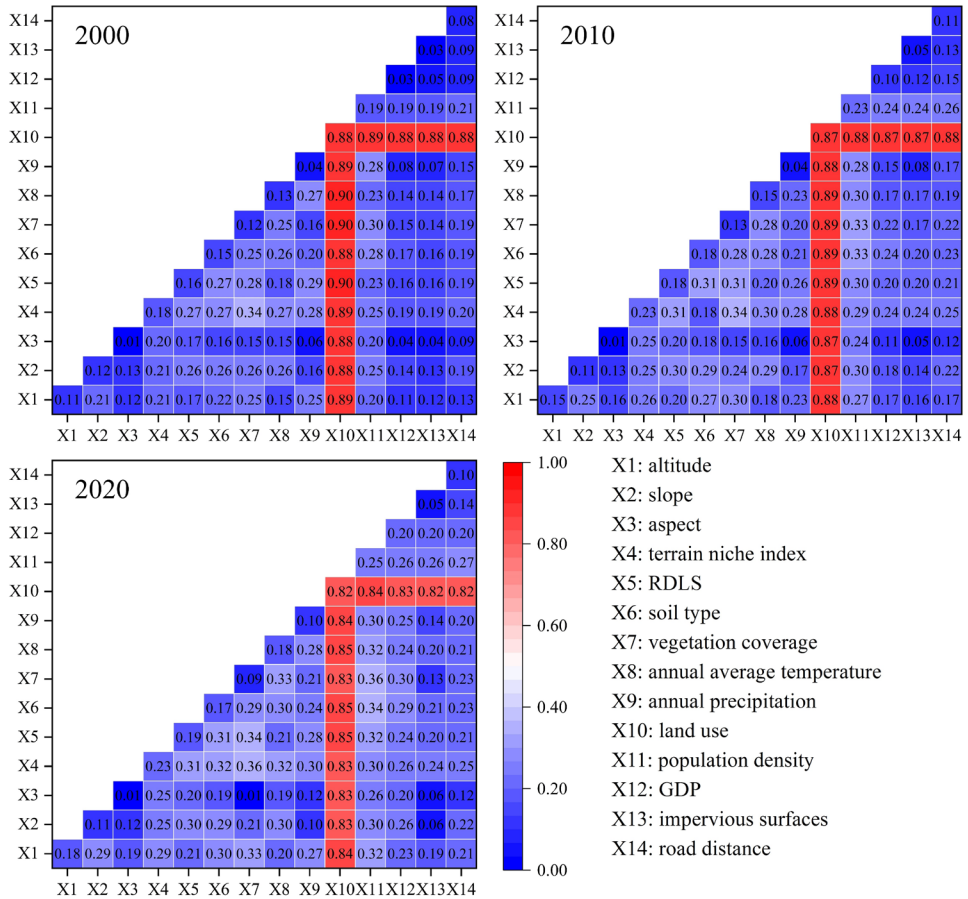

Fig. 7. Interactive detection values of habitat quality factors in the YRB.

compared to the 2000-2010 period. In particular, habitat quality in the Yellow River Delta showed improvement. Over the entire period from 2000 to 2020, the habitat quality index of the YRB initially increased and then stabilized, with some areas maintaining constant habitat quality. Regions experiencing severe degradation were mainly located in the Qilian Mountains, parts of the plains in the lower reaches of the Yellow River, the Guanzhong Basin, and the Taihang Mountains. Areas where habitat quality improved were distributed across the Loess Plateau, the Lanzhou New Area, the Ningxia Plain, and the transitional area of the Mu Us Desert.

Habitat Degradation Analysis

The habitat degradation index was also assessed, with degradation categorized into 5 levels: lower (0), low (0 ~ 0.03), middle (0.03 ~ 0.06), high (0.06 ~ 0.09), and higher (> 0.09). The average degradation indices for 2000, 2010, and 2020 were 0.01653, 0.01650, and 0.01644, respectively, indicating a gradual decrease. This suggests that habitat quality has improved slightly over the study period.

From a spatial distribution perspective, the overall spatial pattern of habitat degradation across the three periods remained relatively stable (Fig. 6). Habitat degradation showed a spatial distribution characterized by "high in the center, low at the periphery, high in the east, and low in the west". Areas with lower habitat degradation were primarily forestland and unused land. Low degradation areas were mostly grassland and water bodies, with a more continuous spatial distribution. Medium degradation areas were mainly cultivated land, while areas with high and higher levels of habitat degradation were construction land and rural residential areas, showing a scattered distribution, primarily located in the lower reaches of the Yellow River. From a temporal perspective, between 2000 and 2020, the areas with lower and middle habitat degradation levels first increased and then stabilized, increasing by 0.56% and 0.61%, respectively. The areas with high and low degradation decreased by 0.17% and 1.07%, respectively. The proportion of areas with high degradation levels was very small, and the changes in these areas were also minimal.

Analysis of Factors Affecting Habitat Quality

The influence of various factors on the habitat quality of the YRB showed significant differences, and the p-values for all influencing factors in different years passed the significance test at the 1% level. According to the diagonal data from the interaction detection diagram (Fig. 7), land use was the dominant factor (q > 0.8), followed by population density, terrain niche index, soil type, and RDLS. Among the topographic factors, the q-values for the terrain niche index and RDLS were higher than those for altitude, slope, and aspect, with aspect having the lowest q-value. For meteorological factors, temperature had a much stronger explanatory power for habitat quality than precipitation. Among the anthropogenic factors, population density had a strong explanatory effect on habitat quality. Additionally, during the study period, as urbanization accelerated, the influence of population density and GDP became more pronounced, indicating that human activities play an increasingly important role in habitat quality changes.

The results from the interaction detection indicated that the interaction between any two influencing factors on the spatial differentiation of habitat quality was stronger than the effect of any individual factors alone, showing patterns of bivariate enhancement and nonlinear enhancement. There was no independent or weakened relationship. The interaction between land use and other factors was relatively strong, suggesting that different land use structures determine the distribution patterns of different ecosystem types. When interacting with other factors, natural factors increased their influence on the spatial distribution of habitat quality, indicating that natural factors play a crucial role in determining habitat quality. The interaction between climatic factors (annual average precipitation and temperature) and land use affected the natural variations in land use. Climatic factors indirectly influence habitat quality by affecting land use patterns. The accelerated urbanization process has damaged high-ecological-value habitats such as forestland and water bodies, as the increasing number of threat sources disrupted the spatial distribution of land use, which in turn impacted habitat quality.

Future Land Use Simulation

Accuracy Validation

Based on land use data from 2000 and 2010, the CA-Markov model within the FLUS framework was used to calculate the number of land use grid cells for 2020. These results were compared with the actual land use in 2020. Across 4 scenarios, the average prediction accuracy of the Markov chain prediction was 0.9192, indicating that the model could accurately predict land use quantities. Furthermore, the FLUS model's simulation of the production-living-ecological space coordination priority scenario for 2020 (Fig. 8) was compared with the actual land use data for 2020. The Kappa coefficient was 0.8927, and the overall accuracy was 0.9253. This demonstrates that the FLUS model has a high degree of accuracy and can effectively reflect future land use conditions in the YRB.

Future Land Use Scenario Analysis

Based on the actual conditions of the YRB, simulations were conducted for the years 2030 (Fig. 9) and 2050 (Fig. 10) under 4 scenarios: production space priority, living space priority, ecological space priority, and production-living-ecological space coordination. The results show significant differences in land use

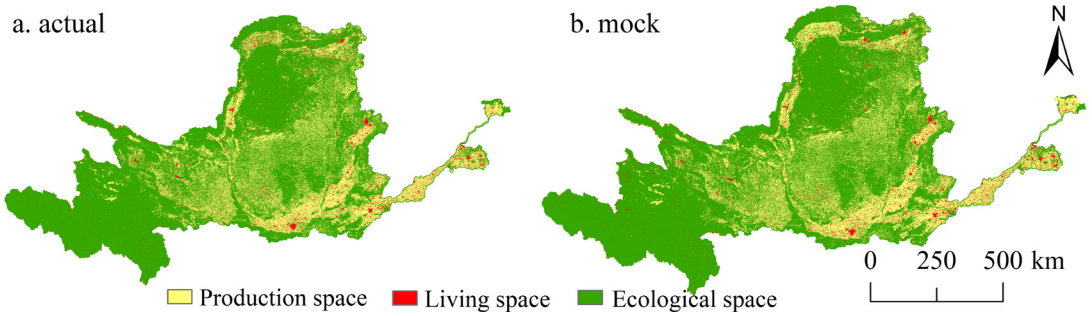

Fig. 8. Land use status and simulation results in the YRB in 2020

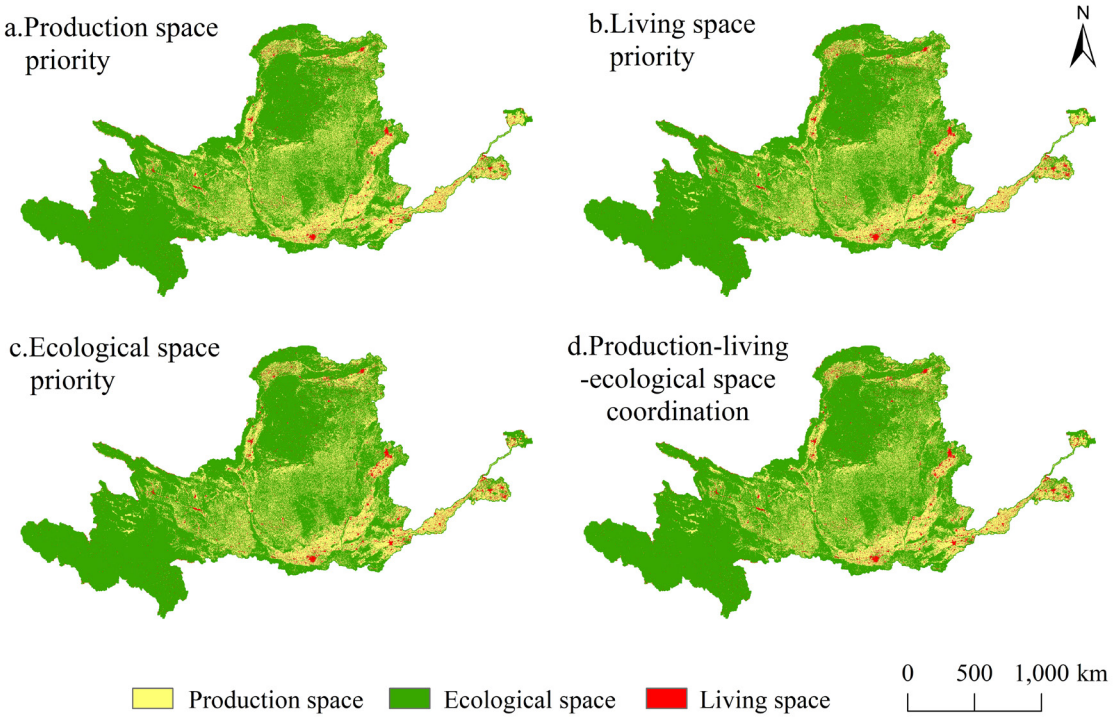

Fig. 9. Simulated prediction of land use in the YRB by 2030 under various sce-narios.

changes and habitat quality between the scenarios. In the production space priority scenario, cultivated land and industrial and mining construction land increase, leading to decreased ecological space. Urban and rural living land expands rapidly in the living space priority scenario, leading to significant habitat degradation. In contrast, the ecological space priority scenario shows an increase in ecological space, particularly in forestland and grassland areas, with habitat quality improving significantly. The production-living-ecological space coordination scenario balances the demands of production, living, and ecological spaces, resulting in moderate improvements in habitat quality.

(1) In the production space priority scenario, forestland, grassland, and unused land are the primary types of land being converted. The main goals of this scenario are to protect cultivated land and ensure sufficient industrial and mining construction land. The model achieves this by increasing the probability of other land types converting to cultivated land and reducing the probability of cultivated land converting to other land types. Additionally, the demand for production space increases by the target years, raising the cost of converting cultivated land to other types. Conversely, the cost of converting other land types into cultivated land, except for urban and rural living land and industrial and mining construction land, is reduced to prioritize production space. From 2020 to 2030, the production space within the "Three-Life Space" of the YRB is projected to increase by 7.02×10^3 km², with cultivated land increasing by 6.97×10^3 km² and industrial and mining construction land increasing by 50 km². The living space will also expand by 1.05×10^2 km², while the ecological space is expected to decrease by 7.13×10^3 km². As production and living spaces continue to grow,

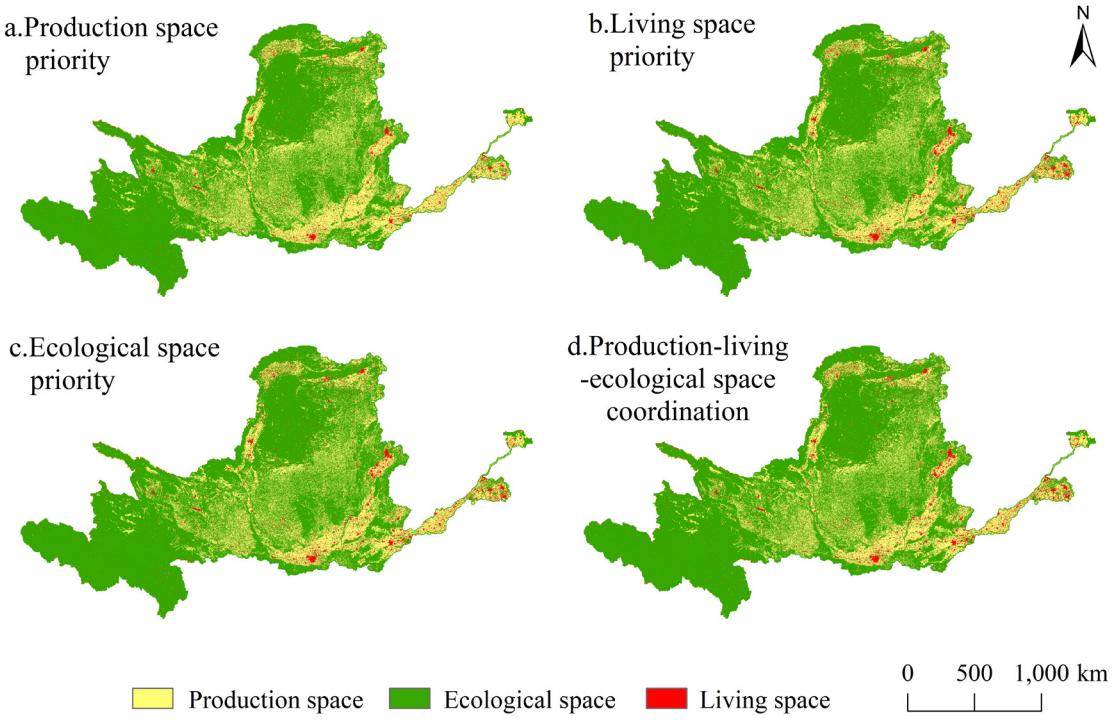

Fig. 10. Simulated prediction of land use in the YRB by 2050 under various scenarios.

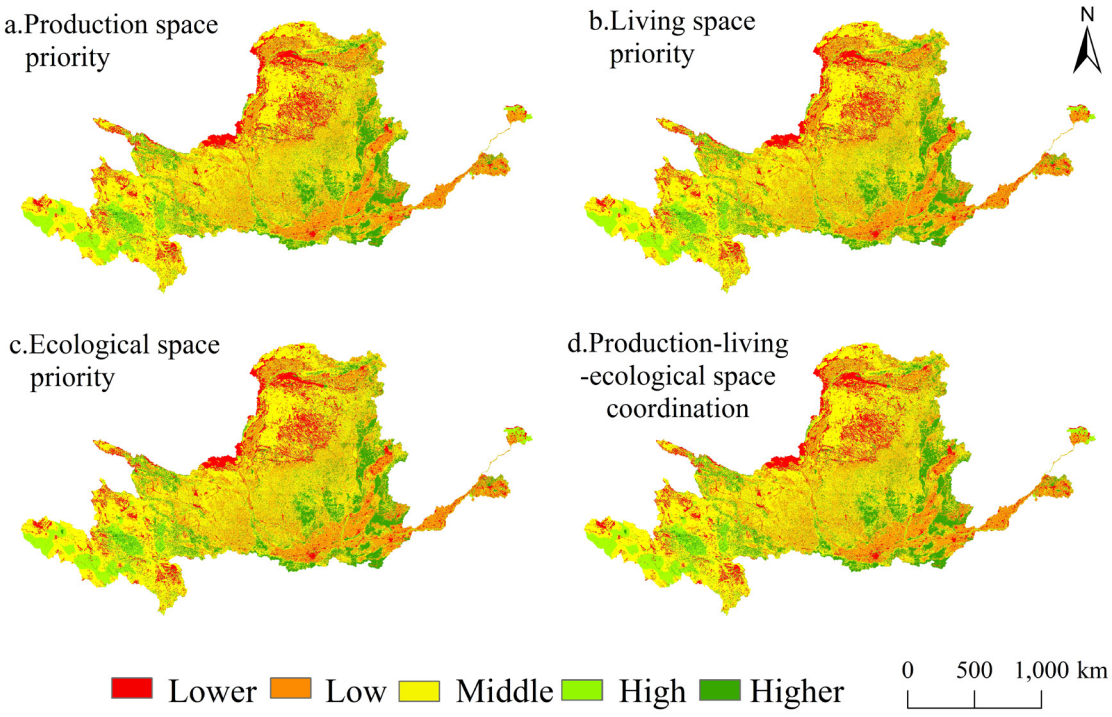

Fig. 11. Habitat quality simulation results in the YRB by 2030 under various scenarios.

ecological space is projected to decrease further by 1.57×10^2 km² between 2030 and 2050;

(2) In the living space priority scenario, cultivated land, grassland, and unused land are the primary land types being converted. The primary land type for living space is urban and rural living land. In the model, this scenario is realized by increasing the probability of other spaces converting to living space while restricting the conversion of living space land types to other categories, achieving the goal of prioritizing living space development. Under this scenario, ecological space continuously decreases. From 2020 to 2030,

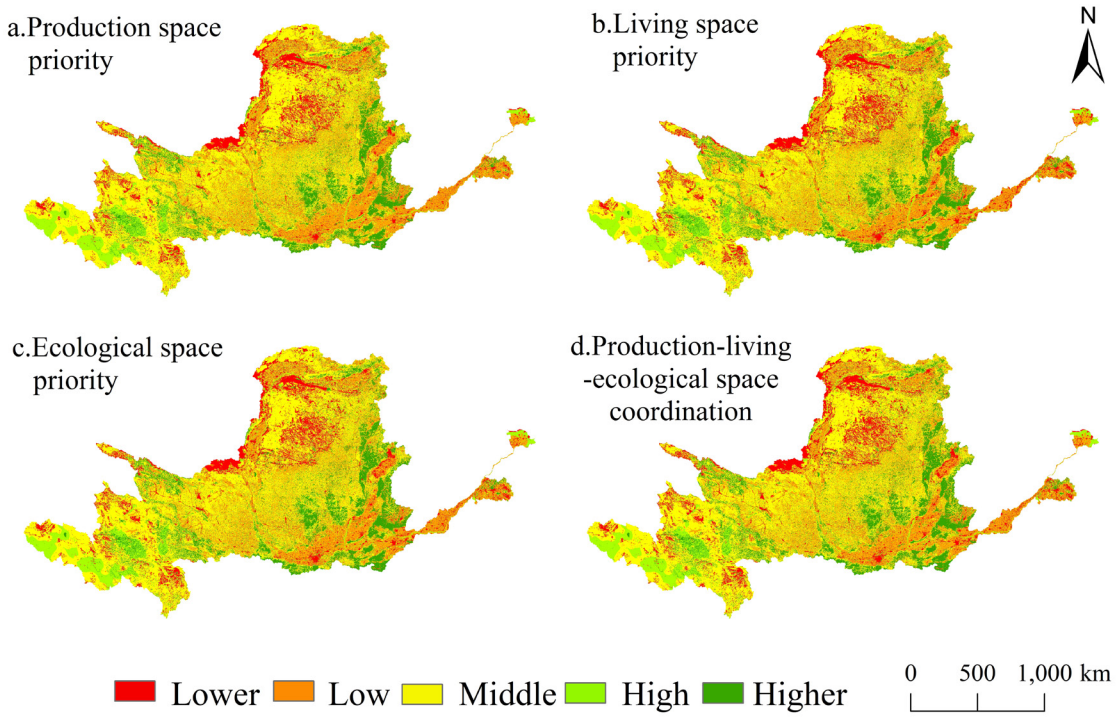

Fig. 12. Habitat quality simulation results in the YRB by 2050 under various scenarios.

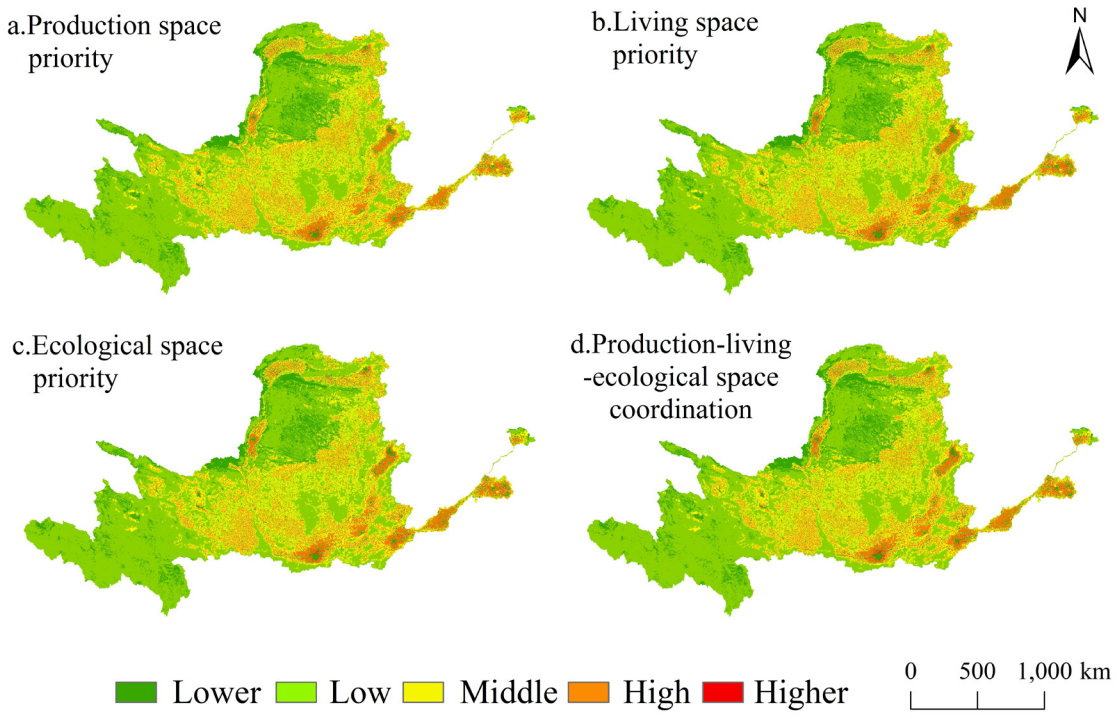

Fig. 13. Simulation results of habitat quality degradation in the YRB by 2030 under various scenarios.

ecological space is expected to decrease by 2.89×10^3 km²; from 2030 to 2050, it will decrease by 1.42×10^2 km². Regarding land expansion capability, industrial and mining construction and urban and rural living land have strong expansion potential with similar land use characteristics. Cultivated land, grassland, and forestland are the main land types being converted. As urban areas expand, on the one hand, the continuous expansion of living space is observed, with an increase of 1.97×10^3 km² in living space from 2020 to 2030 and 3.37×10^3 km² from 2030 to 2050. On the other hand, transportation infrastructure and industrial and mining

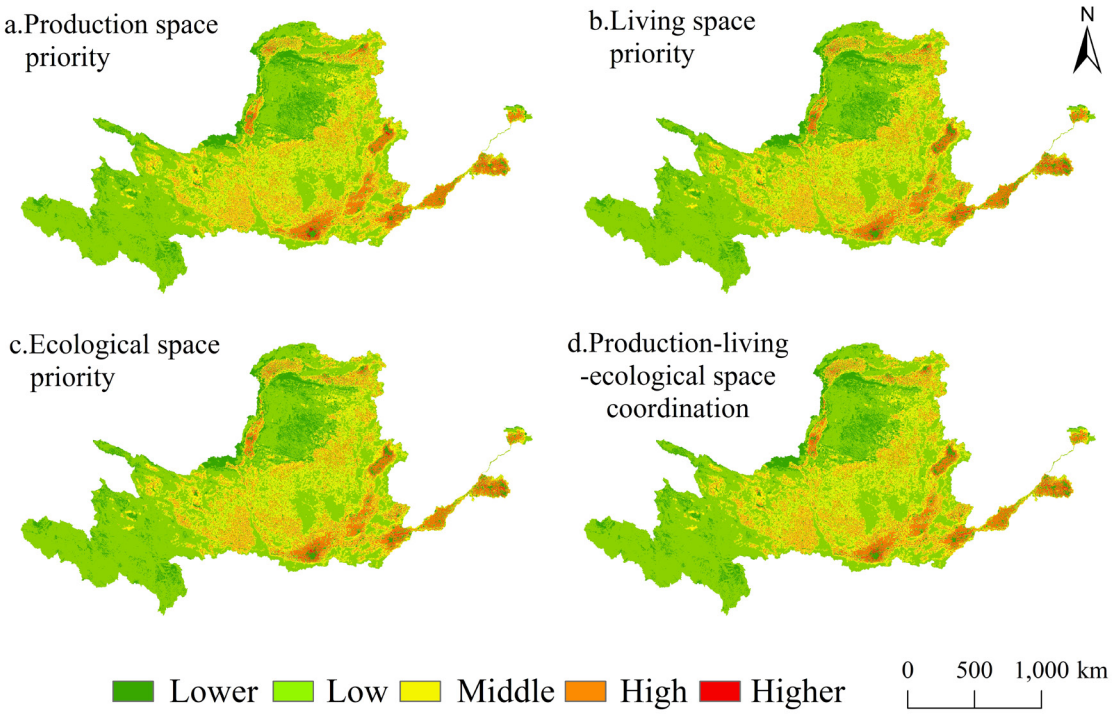

Fig. 14. Simulation results of habitat quality degradation in the YRB by 2050 under various scenarios.

construction land should also increase and improve to facilitate more convenient living conditions. From 2020 to 2030, industrial and mining construction land is projected to increase by 1.33×10^3 km², greater than the decrease in cultivated land by 4.11×10^2 km², resulting in an overall increase in production space. However, from 2030 to 2050, industrial and mining construction land is expected to continue increasing by 1.24×10^3 km², while cultivated land will decrease by 4.47×10^3 km², leading to a slight overall decline in production space;

(3) In the ecological space priority scenario, cultivated and unused land are the primary types being converted. The main goal is to protect ecological space from encroachment while encouraging the conversion of other land types into ecological space to restore ecosystems. The model achieves this by strictly controlling the conversion of ecological space-related land types into living and production space while moderately increasing the conversion of production and living spaces into ecological space. From 2020 to 2030, production space is expected to decrease by 4.3×10^3 km², living space will increase by 1.97×10^3 km², and ecological space will increase by 2.33×10^3 km². From 2030 to 2050, production space is projected to further decrease by 1.75×10^3 km², living space will increase by 3.37×10^3 km², and ecological space will decrease by 1.62×10^3 km². This indicates that production space will become the primary land type being converted under this scenario. Between 2020 and 2030, production space shifted to ecological and living spaces. However, from 2030 to 2050, a large amount of unused land will be converted into living space, leading to an increase in living space and a reduction in ecological space;

(4) The production-living-ecological space coordination scenario shares similar land use conversion patterns with the living space priority scenario, though the changes are somewhat more moderate. This scenario aims to balance the multiple demands of optimizing production space, prioritizing living space, and prioritizing ecological space. The model achieves this by following the principle of conversion costs, increasing the conversion cost for industrial and mining construction land, and controlling the conversion of ecological space land types. The results indicate that the land use area proportions in the production-living-ecological space coordination scenario are very similar to those in the ecological space priority scenario. In terms of area changes, from 2020 to 2030, production space is expected to decrease by 4.27×10^3 km², ecological space will increase by 2.30×10^3 km², and living space will increase by 1.97×10^3 km². From 2030 to 2050, production space is projected to decrease by 1.78×10^3 km², ecological space will decrease by 1.59×10^3 km², and living space will increase by 3.37×10^3 km². The pattern of change is similar to that in the ecological space priority scenario.

Future Habitat Quality and Degradation Analysis

Future Habitat Quality Analysis

The habitat quality of the YRB in 2030 (Fig. 11) and 2050 (Fig. 12) was simulated and evaluated under

4 different scenarios. The results show that ecological space exhibits a growth trend in both the ecological space priority scenario and the production-living-ecological space coordination scenario, while it decreases in the other 2 scenarios. Production space shows a growth trend only in the production space priority scenario and a decreasing trend in the other 3 scenarios, with the decrease being particularly significant. Living space shows a growth trend in all scenarios, but the growth is smaller in the production space priority scenario.

In 2030, the average habitat quality values for the YRB under the 4 scenarios (production space priority, living space priority, ecological space priority, and production-living-ecological space coordination) were 0.52612, 0.52687, 0.52882, and 0.52880, respectively. By 2050, the values were 0.53006, 0.52586, 0.53110, and 0.53111, respectively. Compared to 2020, the average habitat quality in 2030 and 2050 shows variation across different scenarios. In the living space priority scenario, the average habitat quality of the YRB is projected to decline further in the future, while in the production space priority, ecological space priority, and Three-Life Space coordination scenarios, the average habitat quality is expected to improve.

(1) In the production space priority scenario, compared to 2020, the habitat quality index of the YRB improved in both 2030 and 2050. The area of lower habitat quality decreases by 0.3% and 0.95%, respectively, while the area of higher habitat quality increases by 3.31% and 3.32%. As a result, there is a slight improvement in the habitat quality index. However, expanding industrial and mining construction land leads to further degradation of the local ecological environment, causing the habitat quality in 2030 under this scenario to be lower than that of the other scenarios;

(2) In the living space priority scenario, the accelerated urban expansion and rapid socioeconomic development result in a significant increase in urban and rural living land, while other land types experience substantial reductions. This leads to a further increase in lower habitat quality areas, particularly concentrated in the northern part of the YRB and the middle and lower reaches of the river. Compared to 2020, the lower habitat quality area will increase by 0.43% by 2050. Additionally, between 2030 and 2050, habitat quality will decline further, with a decrease of 1.1%;

(3) In the ecological space priority scenario, there is a significant improvement in habitat quality across the region. By 2030 and 2050, the area of higher habitat quality in the YRB will increase by 3.8% and 4.06%, respectively, compared to previous years. The area of lower and low habitat quality decreases. The regions experiencing the greatest increase in higher habitat quality are mainly located in areas where forestland has expanded. Forestland, as a key habitat type, receives better protection under this ecological priority scenario;

(4) In the production-living-ecological space coordination scenario, habitat quality is very similar to that in the ecological space priority scenario. The areas of lower and low habitat quality decrease, while those of higher habitat quality increase.

Overall, the spatial distribution of lower habitat quality areas across the 4 scenarios aligns closely with the distribution of urban and rural living land, industrial and mining construction land, and unused land. This indicates that expanding urban and rural living land, industrial and mining construction land, and unused land directly affect the distribution of lower-value habitat areas within the basin. The distribution of low habitat-quality areas corresponds to the distribution of cultivated land. Additionally, water bodies consistently fall within higher or high habitat quality areas across all scenarios. Although the quantity and spatial distribution of forest land and grassland vary in the simulations under different scenarios, they consistently remain in the higher habitat quality areas.

Future Habitat Degradation Analysis

In 2030, the average habitat degradation index under the 4 scenarios (production space priority, living space priority, ecological space priority, and production-living-ecological space coordination) was 0.02462, 0.02448, 0.02421, and 0.02422, respectively. By 2050, the values were 0.02469, 0.02464, 0.02438, and 0.02439, respectively. Overall, the ranking of habitat degradation is as follows: production space priority > living space priority > production-living-ecological space coordination > ecological space priority. Compared to 2020, the average habitat degradation index in 2030 and 2050 shows variations across the different scenarios.

According to the evaluation results (Fig. 13, Fig. 14), during the periods of 2020-2030 and 2030-2050, the overall changes in habitat degradation were relatively small, but the habitat degradation index showed a gradual increase over time. Although the focus of each simulation differs among the 4 scenarios, the higher habitat degradation areas are consistently concentrated in the eastern part of the basin. These regions have many cities and experienced rapid economic development, leading to significant human disturbance and lower habitat quality. This pattern closely aligns with the spatial distribution of urban and rural living land, indicating that expanding urban-rural residential areas is a key factor driving the increase in lower habitat quality areas. Overall, from 2020 to 2050, the spatial distribution of habitat degradation continues to exhibit the pattern of "high in the center, low at the periphery, high in the east, and low in the west".

Discussion

Response of Habitat Quality to Land Use Change

Our findings showed that the spatial distribution of habitat quality aligns closely with land use patterns, quantitatively confirming that land use ($q > 0.8$) was the

dominant factor influencing the spatial differentiation of habitat quality, consistent with previous studies [34, 44, 47-49]. The higher habitat quality areas were mainly distributed in the southeastern part of the YRB, dominated by forestland. The high-value areas were mainly distributed in the southwest, characterized by forestland, grassland, and water bodies. The middle-value areas were mainly concentrated in the central part of the basin, dominated by grassland. In contrast, lower and low habitat quality areas were concentrated in the east and north, where urban and rural living land, industrial and mining land, and unused land were prevalent.

The average habitat quality values of the YRB ranged from 0.5052 in 2000 to 0.5068 in 2020, showing a trend of overall improvement, albeit with localized deterioration, which is consistent with Fu et al.'s research results [49]. Land-use changes were mainly driven by implementing environmental protection policies and the urbanization process. Frequent human activities will significantly change the regional land use distribution pattern, which in turn affects the regional habitat quality. Our analysis revealed that population density and GDP have increasingly influenced habitat quality, particularly in urban-rural fringe areas, where the conflict between human activities and land resources is most pronounced. From 2000 to 2020, industrial and mining construction land expanded by 379.39%, and urban and rural residential land grew by 36.45%. Urban expansion, especially around large cities, has led to significant habitat degradation [48]. These changes, particularly in the eastern and central regions, were accompanied by a corresponding decline in habitat quality as urban sprawl encroached on natural habitats. Conversely, regions dominated by forestland and grassland, particularly in the western and southern parts of the YRB, showed improved habitat quality. It indicated a sustained trend toward ecological restoration, driven by ongoing reforestation, soil erosion control, and ecological restoration projects [44]. This highlights the critical challenge of harmonizing economic development with ecological conservation to ensure a sustainable trajectory for the basin.

Future Habitat Quality Prediction

The FLUS model used in this study achieved high simulation accuracy, with a Kappa coefficient of 0.8927 and an overall accuracy of 0.9253 when validated against 2020 land use data. Across 4 scenarios, the Markov chain model also demonstrated high predictive accuracy, with an average accuracy of 0.9192. These validation metrics strongly support the future projections made in this study. The ecological space priority scenario shows the most significant improvement in habitat quality, reflecting the positive impact of policy interventions to reduce human disturbance and enhance ecosystem protection. In particular, forest and grassland expansion in ecologically fragile regions demonstrates the effectiveness of ecological protection policies [47]. Nevertheless, the spatial variation in habitat quality between different regions suggests that differentiated strategies are still necessary when implementing policies. In contrast, under the living space priority scenario, habitat quality decreases over time due to the rapid expansion of urban-rural residential areas, emphasizing the need to mitigate the ecological pressure caused by urbanization and socioeconomic development. For future habitat quality to improve, focusing on high-quality development that promotes a harmonious coexistence between humans and nature is crucial. The findings also highlight the value of using scenario-based simulations to inform regional land use planning and ecological protection efforts.

Uncertainties and Challenges for Future Research

Despite the high accuracy of the models and the robust data used, this study has certain limitations. First, land use changes are inherently dynamic and uncertain, influenced by various factors [32, 50]. Future studies should incorporate more factors into the simulations to improve the precision of predictions. Second, while the InVEST model is widely used in habitat quality assessments, the lack of a standardized approach to parameter settings [15] and threat factors introduces potential biases [51, 52]. Further refinement of these parameters, particularly concerning specific human activities and the inclusion of climate change scenarios, will enhance the accuracy of the models in future studies. Additionally, the YRB's vast geographic and climatic variability requires a more granular analysis of habitat quality under different conditions. Comparative studies with other large river basins could provide further insights into the patterns of habitat quality change across different ecological contexts. Strengthening these regional comparisons will be key to understanding how to protect habitat quality under diverse geographic and climatic conditions.

Conclusions

This study employed an integrated modeling framework, coupling FLUS, InVEST, and Geodetector, to analyze historical and future habitat quality dynamics in the ecologically vital YRB. The main conclusions are as follows:

(1) The YRB's landscape was undergoing significant land use transformations characterized by the expansion of industrial and mining construction land and urban and rural living land at the expense of cultivated and unused lands. While grassland remained the dominant cover, these shifts signified intensifying human modification, which fundamentally impacted habitat structure and quality across the basin.

(2) Although the overall average habitat quality in the basin was moderate and exhibited a slight improvement

trend over the past two decades, substantial spatial heterogeneity persisted, generally higher in the west and lower in the east. Habitat degradation pressures are concentrated in the central and eastern regions, intrinsically linked to higher land use intensity and human activity levels, indicating that localized degradation remains a serious concern despite overall trends.

(3) While land use was confirmed as the primary driving factor, anthropogenic pressures (like population density and GDP) were increasingly influential. Crucially, the interactions between different driving factors showed nonlinear enhancement, highlighting the necessity of considering these synergistic effects in environmental management and impact assessments.

(4) Future habitat quality trajectories in the YRB are highly sensitive to policy choices and development pathways. Scenario modeling demonstrates that prioritizing ecological conservation will lead to substantial habitat quality improvements, particularly effective in fragile zones. Conversely, strategies prioritizing rapid expansion of production or living spaces without adequate ecological safeguards will risk significant habitat degradation, primarily through urban and industrial encroachment.

Ultimately, this research underscores the critical role of integrated, spatially explicit modeling in understanding complex human-environment interactions and informing sustainable development. The findings emphasize the profound impact of land use policy on future ecological outcomes and provide vital scientific support for developing targeted conservation strategies, optimizing land use patterns, and balancing development needs with ecological protection imperatives in the YRB.

Conflict of Interest

The authors declare no conflict of interest.

Funding

National Natural Science Foundation of China (41101072, 41671072); Key Scientific Research Project for Higher Education by the Department of Education of Henan Province (23A170020); Shangqiu Science and Technology Innovation Leading Talent Project (SQRC202212005); Henan Provincial Natural Science Foundation (242300420229); Doctoral Scientific Research Start-up Project of Shangqiu Normal University (50018401); Program of Ecological Conservation and High-Quality Development of the Old Course of the Yellow River (2021KYFZ06).

References

1. NEWBOLD T., OPPENHEIMER P., ETARD A., WILLIAMS J.J. Tropical and Mediterranean biodiversity is disproportionately sensitive to land-use and climate change. Nature Ecology & Evolution. **4**, 1630, **2020**.
2. MENGIST W., SOROMESSA T., FEYISA G.L. Landscape change effects on habitat quality in a forest biosphere reserve: Implications for the conservation of native habitats. Journal of Cleaner Production. **329**, 129778, **2021**.
3. WEBER D., SCHAPMAN-STRUB G., ECKER K. Predicting habitat quality of protected dry grasslands using Landsat NDVI phenology. Ecological Indicators. **91**, 447, **2018**.
4. PENG J., PAN Y.J., LIU Y.X., ZHAO H.J., WANG Y.L. Linking ecological degradation risk to identify ecological security patterns in a rapidly urbanizing landscape. Habitat International. **71**, 110, **2018**.
5. DÍAZ S., MALHI Y. Biodiversity: Concepts, patterns, trends, and perspectives. Annual Review of Environment and Resources. **47** (1), 31, **2022**.
6. ZHANG Y., WU T., SONG C.S., HEIN L., SHI F.Q., HAN M.C., OUYANG Z.Y. Influence of climate change and land use change on the interactions of ecosystem services in China's Xijiang River Basin. Ecosystem Services. **58**, 101489, **2022**.
7. JANUS J., BOZEK P. Land abandonment in Poland after the collapse of socialism: over a quarter of a century of increasing tree cover on agricultural land. Ecological Engineering. **138**, 106, **2019**.
8. LI Y.Y., YAO S.B., DENG Y.J., JIA L., HOU M.Y., GONG Z.W. Spatio-temporal study on supply and demand matching of ecosystem water yield service – A case study of Wei River Basin. Polish Journal of Environmental Studies. **30** (2), 1677, **2021**.
9. SALLUSTIO L., TONI A.D., STROLLO A., FEBBRARO M.D., GISSI E., CASELLA L., GENELETTI D., MUNAFÒ M., VIZZARRI M., MARCHETTI M. Assessing habitat quality in relation to the spatial distribution of protected areas in Italy. Journal of Environmental Management. **201**, 129, **2017**.
10. CHEN C.Y., LIU J., BI L.L., Spatial and Temporal Changes of Habitat Quality and Its Influential Factors in China Based on the InVEST Model. Forests. **14**, 374, **2023**.
11. ZHENG H., LI H. Spatial–temporal evolution characteristics of land use and habitat quality in Shandong Province, China. Scientific Reports. **12** (1), 15422, **2022**.
12. LIU Y.X., WANG Y.T., LIN Y.W., MA X.Q., GUO S.F., OUYANG Q.R., SUN C.G. Habitat quality assessment and driving factors analysis of Guangdong Province, China. Sustainability. **15** (15), 11615, **2023**.
13. RIMAL B., SHARMA R., KUNWAR R., KESHTKAR H., STORK N.E., RIJAL S., RAHMAN S.A., BARAL H. Effects of land use and land cover change on ecosystem services in the Koshi River Basin, Eastern Nepal. Ecosystem Services. **38**, 100963, **2019**.
14. XU Y.B., LIU X.H., ZHAO L.R., LI H.Y., ZHU P., LIU R., WANG C., WANG B. Spatial and temporal analysis of habitat quality in the Yellow River Basin based on land-use transition and its driving forces. Land. **14**, 759, **2025**.
15. ANESEYEE A.B., NOSZCZYK T., SOROMESSA T., ELIAS E. The InVEST habitat quality model associated with land use/cover changes: A qualitative case study of the Winike Watershed in the Omo-Gibe Basin, Southwest

Ethiopia. Remote Sensing. **12**, 1103, **2020**.
16. ZHU X.Y., WANG Z.J., GU T.C., ZHANG Y.J. Multi–scenario prediction of land cover changes and habitat quality based on the FLUS–InVEST model in Beijing. Land. **13** (8), 1163, **2024**.
17. QIN X.H., YANG Q.K., WANG L. The evolution of habitat quality and its response to land use change in the coastal China, 1985-2020. Science of the Total Environment. **952**, 175930, **2024**.
18. YU W.Y., JI R.P., HAN X.Z., CHEN L., FENG R., WU J.W., ZHANG Y.S. Evaluation of the biodiversity conservation function in Liaohe Delta wetland, northeastern China. Journal of Meteorological Research. **34** (4), 798, **2020**.
19. JEONG A., KIM M., LEE S. Analysis of priority conservation areas using habitat quality models and MaxEnt models. Animals. **14**, 1680, **2024**.
20. PUGESEK G., CRONE E.E. Contrasting effects of land cover on nesting habitat use and reproductive output for bumble bees. Ecosphere. **12**, e03642, **2021**.
21. GREEN D.B., BESTLEY S., CORNEY S.P., TREBILCO R., LEHODEY P., HINDELL M.A. Modeling Antarctic krill circumpolar spawning habitat quality to identify regions with potential to support high larval production. Geophysical Research Letters. **48**, e2020GL091206, **2021**.
22. SHERROUSE B.C., SEMMENS D.J., ANCONA Z.H. Social Values for Ecosystem Services (SolVES): Open-source spatial modeling of cultural services. Environmental Modelling & Software. **148**, 105259, **2022**.
23. ZHANG K.L., FANG B., ZHANG Z.C., LIU T., LIU K. Exploring future ecosystem service changes and key contributing factors from a "Past-Future-Action" perspective: A case study of the Yellow River Basin. Science of the Total Environment. **926**, 171630, **2024**.
24. WANG B.X., CHENG W.M. Effects of land use/cover on regional habitat quality under different geomorphic types based on invest model. Remote Sensing. **14**, 1279, **2022**.
25. LIU X.P., MA L., LI X., AI B., LI S.Y., HE Z.J. Simulating urban growth by integrating Landscape Expansion Index (LEI) and cellular automata. International Journal of Geographical Information Science. **28**, 148, **2014**.
26. RIMAL B., ZHANG L.F., KESHTKAR H., WANG N., LIN Y. Monitoring and modeling of spatiotemporal urban expansion and land-use/land-cover change using integrated markov chain cellular automata model. ISPRS International Journal of Geo-Information. **6** (9), 288, **2017**.
27. GONG J.Z., HU Z.R., CHEN W.L., LIU Y.S., WANG J.Y. Urban expansion dynamics and modes in metropolitan Guangzhou, China. Land Use Policy. **72**, 100, **2018**.
28. GE X.H., HAN Q.L. Distributed formation control of networked multi-agent systems using a dynamic event-triggered communication mechanism. IEEE Transactions on Industrial Electronics. **64**, 8118, **2017**.
29. LI X., CHEN G.Z., LIU X.P., LIANG X., WANG S.J., CHEN Y.M., PEI F.S., XU X.C. A new global land-use and land-cover change product at a 1 km resolution for 2010 to 2100 based on human-environment interactions. Annals of the American Association of Geographers. **107** (5), 1040, **2017**.
30. LIU X.P., LIANG X., LI X., XU X.C., QU J.P., CHEN Y.M., LI S.Y., WANG S.J., PEI F.S. A future land use simulation model (FLUS) for simulating multiple land use scenarios by coupling human and natural effects. Landscape Urban Plann. **168**, 94, **2017**.
31. TATENDA D., TONGAYI M., WASSERMAN R.J., MADZIVANZIRA T.C., TAMUKA N., CUTHBERT R.N. Land use effects on water quality, habitat, and macroinvertebrate and diatom communities in African highland streams. Science of the Total Environment. **846**, 157346, **2022**.
32. GOMES E., INÁCIO M., BOGDZEVI K., KALINAUSKAS M., KARNAUSKAITE D., PEREIRA P. Future land-use changes and its impacts on terrestrial ecosystem services: a review. Science of the Total Environment. **781**, 146716, **2021**.
33. HUANG C.B., CHENG X.J., ZHANG Z.M. Future land use and habitat quality dynamics: Spatio-temporal analysis and simulation in the Taihu Lake Basin. Sustainability. **16** (17), 7793, **2024**.
34. YIN D.Y., LI X.S., LI G.E., ZHANG J., YU H.C. Spatio-temporal evolution of land use transition and its eco-environmental effects: A case study of the Yellow River Basin, China. Land. **9** (12), 514, **2020**.
35. CHEN G., ZUO D.P., XU Z.X., WANG G.Q., HAN Y.N., PENG D.Z., PANG B., ABBASPOUR K.C., YANG H. Changes in water conservation and possible causes in the Yellow River Basin of China during the recent four decades. Journal of Hydrology. **637**, 131314, **2024**.
36. SUN H.Y., DI Z.H., SUN P.L., WANG X.Y., LIU Z.W., ZHANG W.J. Spatiotemporal differentiation and its attribution of the ecosystem service trade-off/synergy in the Yellow River Basin. Land. **13** (3), 369, **2024**.
37. HUANG M.Y., YUE W.Z., FENG S.R., ZHANG J.H. Spatial-temporal evolution of habitat quality and analysis of landscape patterns in Dabie Mountain area of west Anhui Province based on InVEST model. Acta Ecologica Sinica. **40** (9), 2895, **2020**.
38. PAN W., WANG J., LI Y.R., CHEN S.T., LU Z. Spatial pattern of urban-rural integration in China and the impact of geography. Geography and Sustainability. **4** (4), 404, **2023**.
39. WANG B.X., CHENG W.M. Effects of land use/cover on regional habitat quality under different geomorphic types based on InVEST model. Remote Sensing. **14**, 1279, **2022**.
40. SHARP R., RICKETTS T., GUERRY A.D. InVEST 3.2.0 Beta User's Guide. The Natural Capital Project. Stanford University: Stanford, CA, USA, **2015**.
41. NAIMI B., HAMM N.A.S., GROEN T.A., SKIDMORE A.K., TOXOPEUS A.G., ALIBAKHSHI S. ELSA: Entropy-based local indicator of spatial association. Spatial Statistics. **29**, 66, **2019**.
42. ZHANG X.R, ZHOU J., LI G.N., CHEN C., LI M.M. Spatial pattern reconstruction of regional habitat quality based on the simulation of land use changes from 1975 to 2010. Journal of Geographical Sciences. **30** (4), 601, **2020**.
43. SUN X.Y., JIANG Z., LIU F., ZHANG D.Z. Monitoring spatio-temporal dynamics of habitat quality in Nansihu Lake Basin, eastern China, From 1980 to 2015. Ecological Indicators. **102**, 716, **2019**.
44. SONG Y.N., WANG M., SUN X.F., FAN Z.M. Quantitative assessment of the habitat quality dynamics in Yellow River Basin, China. Environmental Monitoring and Assessment. **193**, 614, **2021**.
45. WANG J.F., ZHANG T.L., FU B.J. A measure of spatial stratified heterogeneity. Ecological Indicators. **67**, 250, **2016**.
46. WANG J.F., HAINING R., ZHANG T.L., XU C.D., HU M.G., YIN Q., LI L.F., ZHOU C.H., LI G.Q., CHEN H.Y. Statistical modeling of spatially stratified heterogeneous data. Annals of the American Association of Geographers. **114** (3), 499, **2024**.
47. LOU Y.Y., YANG D., ZHANG P.Y., ZHANG Y., SONG

M.L., HUANG Y.C., JING W.L. Multi-scenario simulation of land use changes with ecosystem service value in the Yellow River Basin. Land. **11**, 992, **2022**.
48. TANG J.J., ZHOU L., DANG X.W., HU F.N., YUAN B., YUAN Z.F., WEI L. Impacts and predictions of urban expansion on habitat quality in the densely populated areas: A case study of the Yellow River Basin, China. Ecological Indicators. **151**, 110320, **2023**.
49. FU C., LIU Y.Z., CHEN Y.D., LI F., HUANG J.Y., HUANG H.M. Simulation of land use change and habitat quality in the Yellow River Basin under multiple scenarios. Water. **14**, 3767, **2022**.
50. AKSOY H., KAPTAN S. Simulation of future forest and land use/cover changes (2019–2039) using the cellular automata-Markov model. Geocarto International. **37** (4), 1183, **2020**.
51. TANG F., FU M.C., WANG L., ZHANG P.T. Land-use change in Changli county, China: Predicting its spatio-temporal evolution in habitat quality. Ecological Indicators. **117**, 106719, **2020**.
52. RAJI S.A., ODUNUGA S., FASONA M. Spatially explicit scenario analysis of habitat quality in a tropical semi–arid zone: Case study of the Sokoto–Rima Basin. Journal of Geovisualization and Spatial Analysis. **6**, 1, **2022**.